

## 2D homonuclear correlation $^1\text{H}$ solid-state NMR by wPMLG

Product used : nuclear magnetic resonance (NMR)

Multidimensional correlation NMR spectroscopies, which provides inter-nuclear proximity/connectivity, play a crucial role to probe the atomic resolution structures. Especially,  $^1\text{H}$ - $^1\text{H}$  homonuclear correlation spectroscopy is quite useful source of information because of high abundance (>99%) and gyromagnetic ratio, thus resulting in strong inter nuclear interactions. Thanks to the development of high resolution  $^1\text{H}$  solid-state NMR, now it is feasible to observe  $^1\text{H}$ - $^1\text{H}$  correlation high resolution solid-state NMR [1]. There are two distinctive categories; 1) single quantum (SQ)/SQ correlation and 2) double quantum (DQ)/SQ correlations. In this note we introduce 2D  $^1\text{H}$  SQ/ $^1\text{H}$  SQ and  $^1\text{H}$  DQ/ $^1\text{H}$  SQ correlation spectroscopy to probe the internuclear proximity using high-resolution  $^1\text{H}$  solid-state NMR techniques.

### $^1\text{H}$ SQ/ $^1\text{H}$ SQ correlations

SQ coherence is observed in the indirect  $t_1$  dimension, thus essentially the same spectra appear in both dimensions. This makes spectral interpretation straightforward. The connectivity can be read from the off-diagonal cross peaks. The sequence is essentially the same as NOESY experiments, but wPMLG is applied during the  $t_1$  and  $t_2$  dimensions to achieve  $^1\text{H}$ - $^1\text{H}$  decoupling during spin evolution (Fig 1). The first pulse excites the SQ coherence. Followed by the  $t_1$  evolution, the magnetization is stored along the z-axis by the second 90 degree pulse. The  $^1\text{H}$  magnetization is diffused to the other  $^1\text{H}$ s during the mixing time. Finally, the magnetization is observed during  $t_2$  after third 90 degree pulse. In this approach,  $^1\text{H}$ - $^1\text{H}$  correlation is established during the mixing time between the indirect SQ and direct SQ dimensions. As the magnetization stored along the z-axis, one can elongate mixing time to the order of  $^1\text{H}$   $T_{1\rho}$ , allowing multiple relayed coherence transfer, or spin diffusion. Thus, SQ/SQ can potentially provide long range ( $\sim 100$  Å) correlations. In addition, the semi-quantitative distance measurement can be achieved by monitoring of build up of correlation peaks. Typically the build up curve is evaluated with empirical spin diffusion equation [2], however, explicit spin dynamic calculation can also be applied [3]. One drawback is presence of uncorrelated peak on the diagonal line. This hampers the observation of correlations between the nuclei possessing identical or very close chemical shifts.

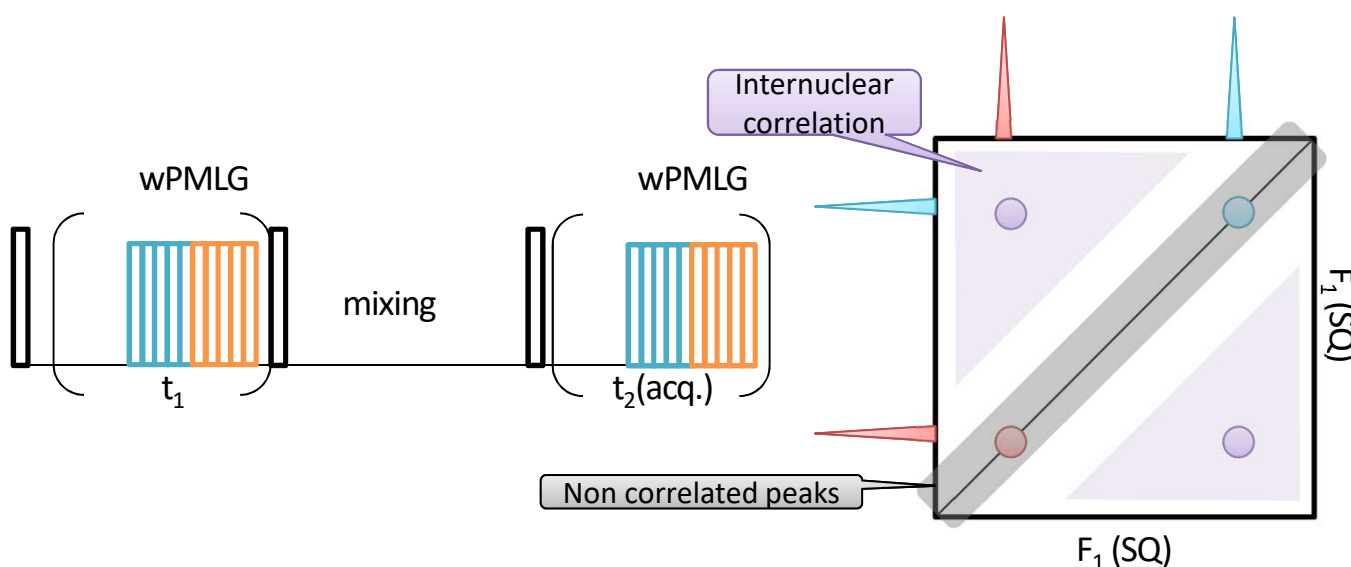


Fig 1. Pulse sequence (left) and schematic representation of  $^1\text{H}$  SQ/ $^1\text{H}$  SQ correlation spectrum (right).



### $^1\text{H}$ SQ/ $^1\text{H}$ SQ correlations: experimental setup

wPMLG decoupling is optimized by spin echo experiments. We recommend z-rotation wPMLG supercycling to avoid the necessity of trim pulses. As no acquisition window is required in the indirect dimension, windowless PMLG or the other windowless  $^1\text{H}$ - $^1\text{H}$  decoupling sequences can be used during  $t_1$ . However, this introduces different scaling factor in the  $t_1$  dimension than that in  $t_2$ , complicating processing. Here we recommend to use the same  $^1\text{H}$  decoupling sequence as the  $t_2$  dimension for the sake of simplicity. The indirect spectral width is automatically synchronized to the wPMLG block, and defined by LG\_Loop in the pulse program. The signal is sampled every LG\_Loop times of wPMLG block in the indirect dimension. By maximizing LG\_LOOP or minimizing indirect spectral width, one can reduce the experimental time. One can easily optimize the minimum indirect spectral width by investigating the 1D wPMLG spectrum. As 1D wPMLG spectrum is sampled every wPMLG block, the spectral width is automatically set as  $1/\text{cycle\_time}$ . Thus the spectral range is from  $-1/(2 \times \text{cycle\_time})$  to  $+1/(2 \times \text{cycle\_time})$ . If the peaks appear only between  $-1/(n \times 2 \times \text{cycle\_time})$  to  $+1/(n \times 2 \times \text{cycle\_time})$ , one can safely sample signal every  $n \times \text{cycle\_time}$  of wPMLG. As shown in Fig 2, LG\_LOOP = 4 is wide enough to cover the spectral range in this case. However, the artifacts which appear in the outside the peak area will be folded into the spectral range by setting LG\_LOOP larger than one. Thus, if time allows, LG\_LOOP = 1 is preferable to avoid complexity. Since  $^1\text{H}$ - $^1\text{H}$  spin diffusion is rapid enough at moderate MAS rate, no rf field is applied during the mixing time in most cases. However, recoupling/decoupling sequence can be applied if needed [4]. As the mixing time works as z-filter, or in other words, residual transversal magnetization is suppressed during the mixing time, 2 step phase cycling is enough for coherence pathway selection. In case of zero or very short mixing time, additional 3 step phase cycling, which makes the total 6-step phase cycling, is needed to suppress transversal magnetization during the mixing time. While long mixing time can be used to diffuse  $^1\text{H}$  magnetization to remote  $^1\text{H}$ s, the mixing time has to be shorter than  $^1\text{H}$   $T_1$ . Otherwise the signal will be lost.

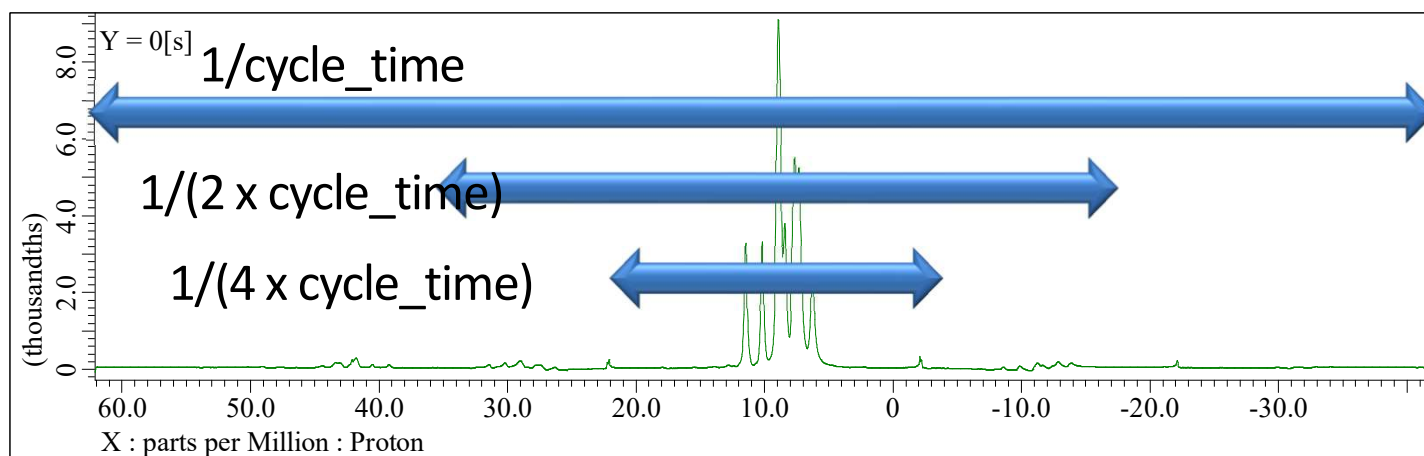


Fig 2.

$^1\text{H}$  wPMLG spectrum of L-tyrosine.HCl at 12 kHz under 14.1 T. The spectral width is automatically set to  $1/\text{cycle\_time}$ . As all the peak appear in  $-1/(4 \times 2 \times \text{cycle\_time})$  to  $+1/(4 \times 2 \times \text{cycle\_time})$ , the sampling every four cycle time of wPMLG is enough to cover all the spectral area in the indirect dimension of  $^1\text{H}$  SQ/ $^1\text{H}$  SQ correlation spectra.



## $^1\text{H}$ SQ/ $^1\text{H}$ SQ correlations: data processing

The direct dimension is the same as 1D wPMLG. Linear\_Ref and Reference should be applied to correct chemical shift scalings. As the indirect dimension represents SQ chemical shift, the same scaling can be applied. Fig 3 shows the resultant 2D spectrum and process list used.

## Pulse program: wpmlg5\_exchange\_2d.jxp

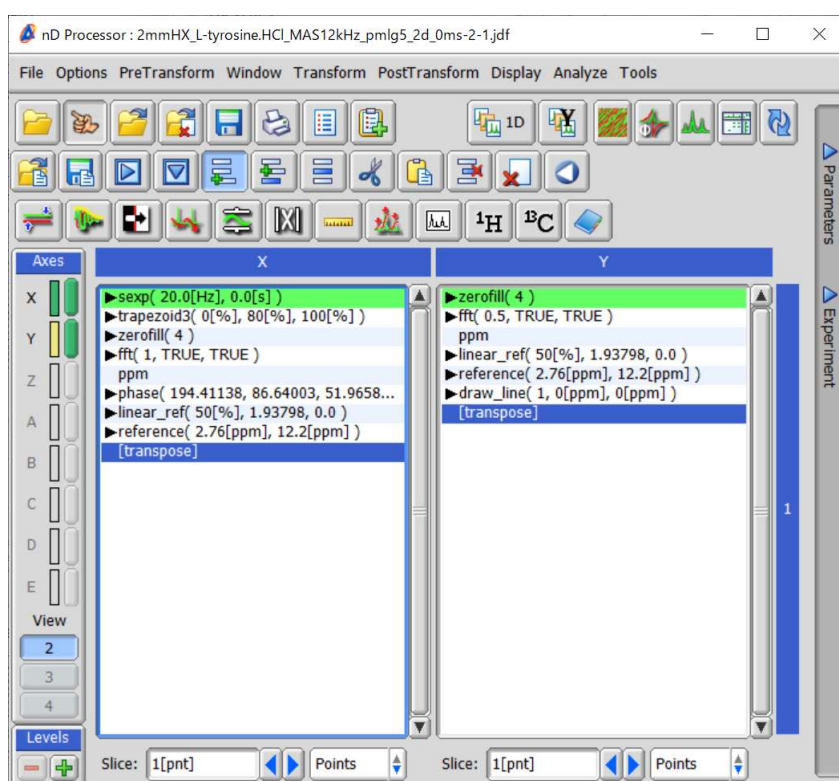
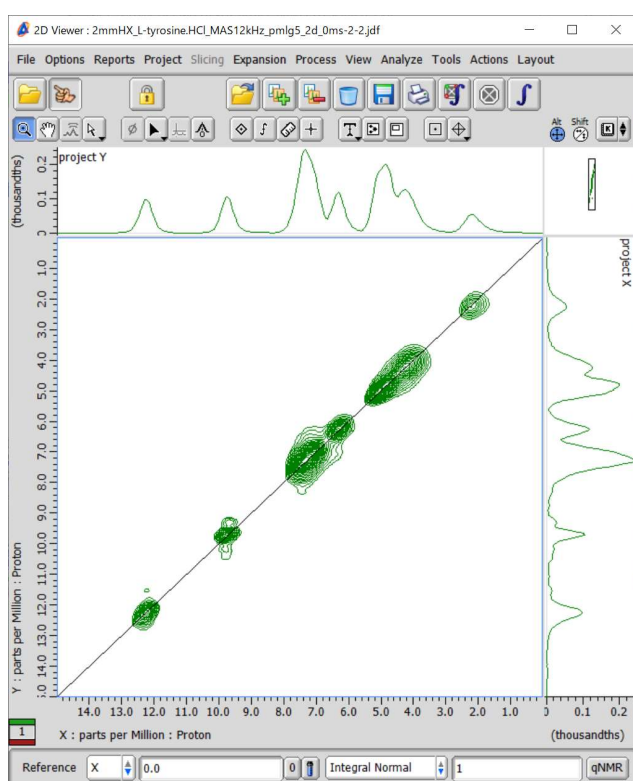
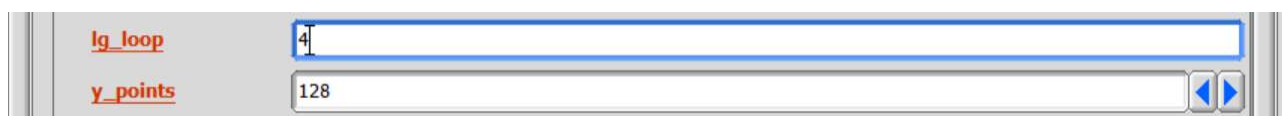


Fig 3.

$^1\text{H}$  SQ/ $^1\text{H}$  SQ correlation spectrum of L-tyrosine.HCl at 12 kHz under 14.1 T (left). wPMLG decoupling is applied to both  $t_1$  and  $t_2$  dimensions. No mixing time is used (mixing time = 0). The process list is basically the same as regular 2D but Linear\_Ref and Reference function should be applied to the both dimension (right). The increment of the indirect dimension is set to four times of the wPMLG cycle time by putting Lg\_loop = 4. 128  $t_1$  points were collected with 6cans for each. The total measurement time was  $128 \times 6 \times 2 \times 1.5 \text{ s}$  (repetition delay) = 39 mins.

No correlation peaks appear in Fig 3, because of devoid of mixing time. However, even very short mixing time of 50  $\mu$ s introduces cross peaks between neighboring  $^1\text{H}$ s (Fig 4a). The intensities of cross peaks rapidly grow as the mixing time. (Fig 4b and c). The analysis of build up provides semi-quantitative distance information between  $^1\text{H}$ s.

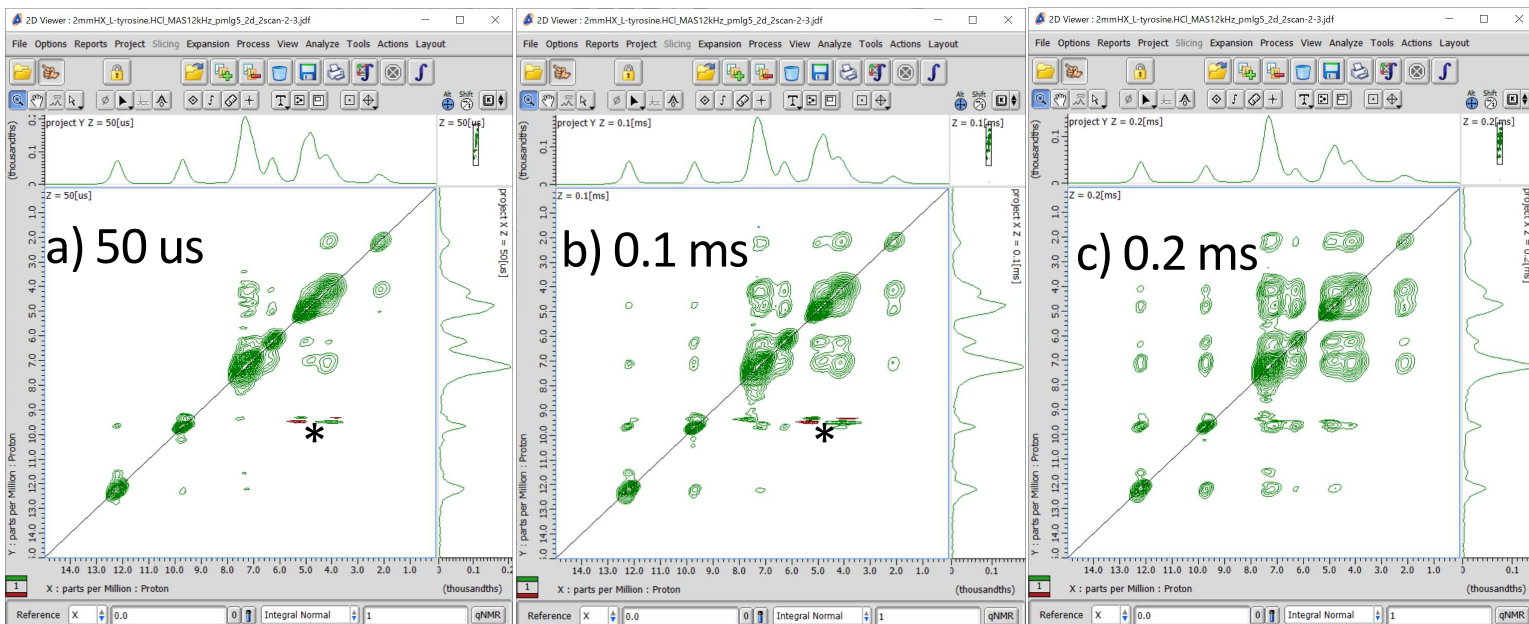


Fig 4.  $^1\text{H}$  SQ/ $^1\text{H}$  SQ correlation spectrum of L-tyrosine.HCl at 12 kHz under 14.1 T at a mixing time of 50  $\mu$ s (a), 0.1 ms (b) and 0.2 ms (c). The glitch marked asterisk is artifact appearing at the center of the indirect dimension. The increment of the indirect dimension is set to four times of the wPMLG cycle time by putting  $Lg\_loop = 4$ . 128  $t_1$  points were collected with 2cans for each. The total measurement time was  $128 \times 2 \times 1.5$  s (repetition delay) = 13 mins for each.



**<sup>1</sup>H DQ/ <sup>1</sup>H SQ correlations**

Proximity between <sup>1</sup>Hs can be monitored by <sup>1</sup>H DQ/<sup>1</sup>H SQ correlation spectroscopy as well (Fig 5). Unlike <sup>1</sup>H SQ/<sup>1</sup>H SQ correlation, <sup>1</sup>H DQ/<sup>1</sup>H SQ correlation gives very local proximity below < 4Å, and is useful to probe the atomic resolution structure. In this experiments, first DQ coherence is created by the DQ excitation block. The DQ coherence is evolved during t<sub>1</sub> period under wPMLG irradiation. Then it is converted to longitudinal magnetization by the DQ reconversion block. A soft z-filter could be inserted before the final read 90 degree pulse. Finally, SQ coherence is observed under wPMLG decoupling. The close similarity to <sup>1</sup>H SQ/<sup>1</sup>H SQ sequence can be found. In fact, DQ/SQ sequence can be described by replacing the first and second 90 degree pulse in SQ/SQ to DQ excitation and reconversion blocks, respectively. The major difference is mechanism to establish <sup>1</sup>H-<sup>1</sup>H correlation. While SQ/SQ experiments utilize <sup>1</sup>H-<sup>1</sup>H spin diffusion during the mixing time, the two spin DQ coherences which are created by the DQ excitation block reports the two spin proximities in DQ/SQ experiments. The dipolar truncation during the DQ recoupling hampers the creation of DQ coherence between remote spins. Thus only short (typically < 4 Å) <sup>1</sup>H proximity is observed. All the correlation appear in DQ/SQ spectra come from two spin connectivities in 4 Å. No uncorrelated peaks appear. This makes spectral interpretation simple. The schematic 2D DQ/SQ spectrum is shown in Fig 5. Two peaks appear at ω<sub>A</sub> and ω<sub>B</sub> in the SQ dimension. The correlation between like spin between A and A appear at ω<sub>A</sub> + ω<sub>A</sub> = 2ω<sub>A</sub> in the indirect dimension, thus (DQ, SQ) = (2ω<sub>A</sub>, ω<sub>A</sub>). For this reason, diagonal line is plotted with a slope of 2 passing at (0, 0) ppm. The devoid of correlation at (DQ, SQ) = (2ω<sub>A</sub>, ω<sub>A</sub>) shows that B doesn't have like spin in close distance. The correlation between A and B appears at (DQ, SQ) = (ω<sub>A</sub> + ω<sub>B</sub>, ω<sub>A</sub>) and (ω<sub>A</sub> + ω<sub>B</sub>, ω<sub>B</sub>) with equidistance from the diagonal line.

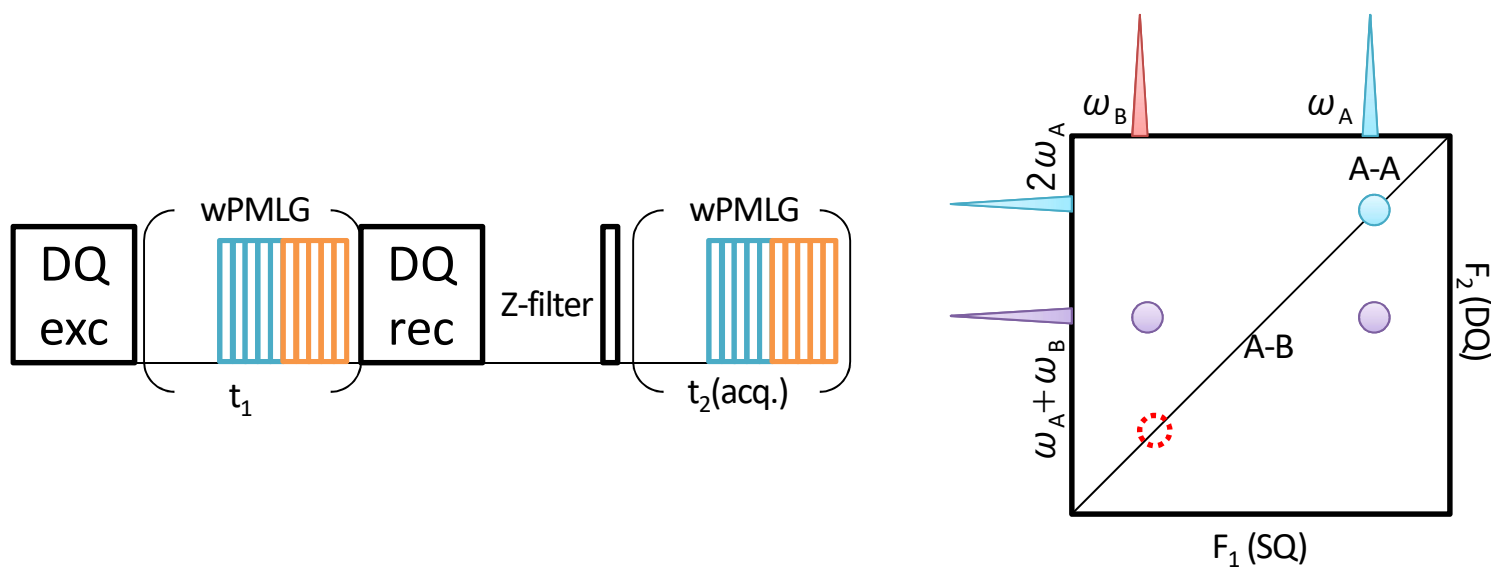


Fig 5. Pulse sequence (left) and schematic representation of <sup>1</sup>H DQ/<sup>1</sup>H SQ correlation spectrum (right). All the peaks appearing in the spectra are correlated peaks.

Certain products in this brochure are controlled under the "Foreign Exchange and Foreign Trade Law" of Japan in compliance with international security export control. JEOL Ltd. must provide the Japanese Government with "End-user's Statement of Assurance" and "End-use Certificate" in order to obtain the export license needed for export from Japan. If the product to be exported is in this category, the end user will be asked to fill in these certificate forms.

**<sup>1</sup>H DQ/ <sup>1</sup>H SQ correlations: experimental setup**

The same wPMLG block with z-rotation is applied during both  $t_1$  and  $t_2$  periods. Although any <sup>1</sup>H DQ recoupling scheme, in principle, can be used for excitation and reconversion periods, we recommend POST-C7 because of robustness to experimental imperfections and its gamma-encoded nature [5,6]. As POST-C7 require rf-field strength seven times of the MAS rate, maximum MAS rate is often limited by the <sup>1</sup>H rf-field capability of the probe. For example, the probe which can accept 100 kHz <sup>1</sup>H irradiation accommodates POST-C7 at 100/7 = 14.3 kHz MAS rate. Thus, MAS rate has to be carefully chosen so that POST-C7 can be applied. POST-C7 has only one parameter to be optimized, i.e. rf-field strength. The experimental optimization can be done by comparing 1D spectra at  $t_1 = 0$  with varying rf field strength (obs\_amp\_c7). (Fig 6) As POST-C7 is quite robust to rf field strength variation, no need to fine step tuning. We typically vary every 5 kHz or so. The DQ filtering efficiency compared to regular 1D wPMLG is typically found in 5-20% for rigid solids. It should be noted that the peaks in the indirect DQ dimension appears not at the center, but at the spinning sideband position due to DQ recoupling mechanism. [7] POST-C7 recouples  $m = 1$  terms in the gamma-encoded manner, thus the peak appears at the +1 SSB positions, or in other words, all the peaks shifted with the MAS rate toward high frequency side (Fig 7). Thus the peak positions can be easily corrected by simply shifting the peak position with the MAS rate. Any MAS rate can be used in case of POST-C7 as long as probe accept the rf field strength. The peak position in the indirect dimension can be predicted including +MAS frequency shift. However, it is a bit complicated. Thus, we recommend to use widest spectral range with LG\_LOOP = 1, if time allows. Instead, one can repeat quick 2D experiments varying LG\_LOOP so that all the peaks fit in the indirect spectral range. During this optimization, z-filter can be used at z-filter doesn't alter the spectral range in the indirect dimension. This allows 4-step phase cycling, shortening the experimental time. [Non-gamma encoded DQ recoupling sequences poses additional difficulty that the indirect spectral width has to be the same as MAS rate as discussed below. For this reason, we recommend gamma-encoded sequence. Non-gamma encoded sequences give peaks at +/-1 or 2 SSB positions, giving additional splittings. In order to avoid the splitting, the spectral width of indirect dimension has to be synchronized to the MAS rate. When the spectral width is the same as the MAS rate, all the DQ peaks folded back onto the center band. This approach is frequently used at fast MAS, avoiding complexity of peak shiftings. However, this also poses additional problem of limited spectral width especially at moderate MAS rate. For example, 12 kHz spectral width corresponding to 20 ppm at 14.1 T, which is not enough to cover entire range of <sup>1</sup>H DQ spectra.]

**Pulse program: postc7\_wpmlg5\_2d.jxp**  
**Criterion: maximize the intensity**

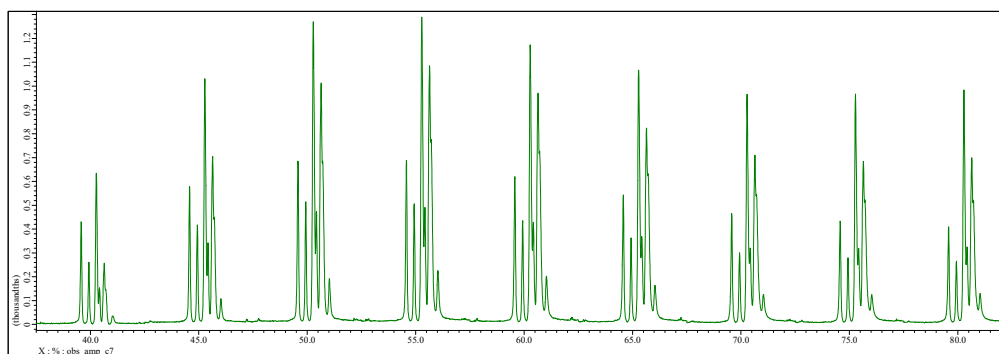
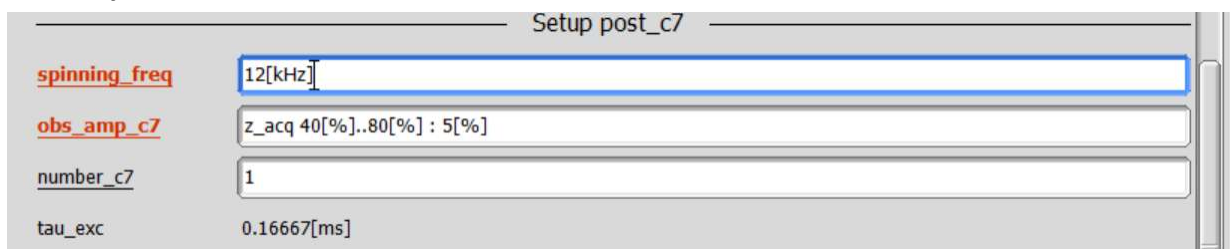


Fig 6. DQ filtered <sup>1</sup>H spectra of L-tyrosine.HCl at 12 kHz and 14.1 T observed at various rf field strength for POST-C7. The spectra were observed using the sequence in Fig 5 with  $t_1 = 0$ . While nominal rf field strength for POST-C7 is seven times of the MAS rate, the maximum DQ efficiency may appear at the slightly different rf field strength.

Certain products in this brochure are controlled under the "Foreign Exchange and Foreign Trade Law" of Japan in compliance with international security export control. JEOL Ltd. must provide the Japanese Government with "End-user's Statement of Assurance" and "End-use Certificate" in order to obtain the export license needed for export from Japan. If the product to be exported is in this category, the end user will be asked to fill in these certificate forms.

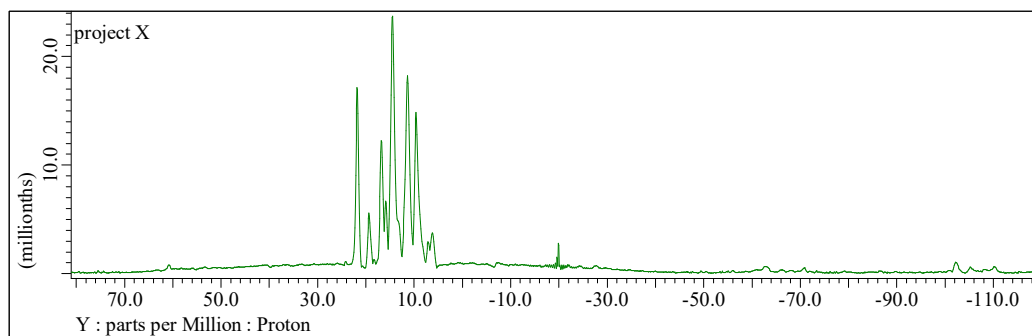


Fig 7. Projection onto the DQ dimension of DQ/SQ correlation spectra of L-tyrosine.HCl at MAS rate of 12 kHz and 14.1T. POST-C7 is utilized to excite/reconvert DQ coherences. The DQ peaks appear not at the center but at +1 SSB positions.

Z-filter can be used to suppress transversal magnetization, making total number of step is 4 scans. However, it is advisable to use zero-z-filter to avoid spin diffusion during the z-filter. In this case, we need 12-step phase cycling for coherence selection. Fig 8 demonstrates the effect of spin diffusion during z-filtering. In the absence of z-filtering, regular <sup>1</sup>H DQ/<sup>1</sup>H SQ patterns appear (Fig 8a). However, the insertion of 1 ms z-filter results in many additional peaks which are coming from spin diffusion (Fig 8b). As evident from Fig 4, a fraction of millisecond is enough to cause <sup>1</sup>H-<sup>1</sup>H spin mixing at moderate MAS rate, deteriorating the <sup>1</sup>H DQ/<sup>1</sup>H SQ spectra. We recommend not to use z-filtering to avoid this complexity.

Care must be taken for acquisition time. As rf field is almost continuously applied during excitation, t<sub>1</sub>, reconversion, and t<sub>2</sub> period, the total duration has to be shorter than 50 ms to avoid probe failure. Be careful of x\_acq\_time and y\_acq\_time.

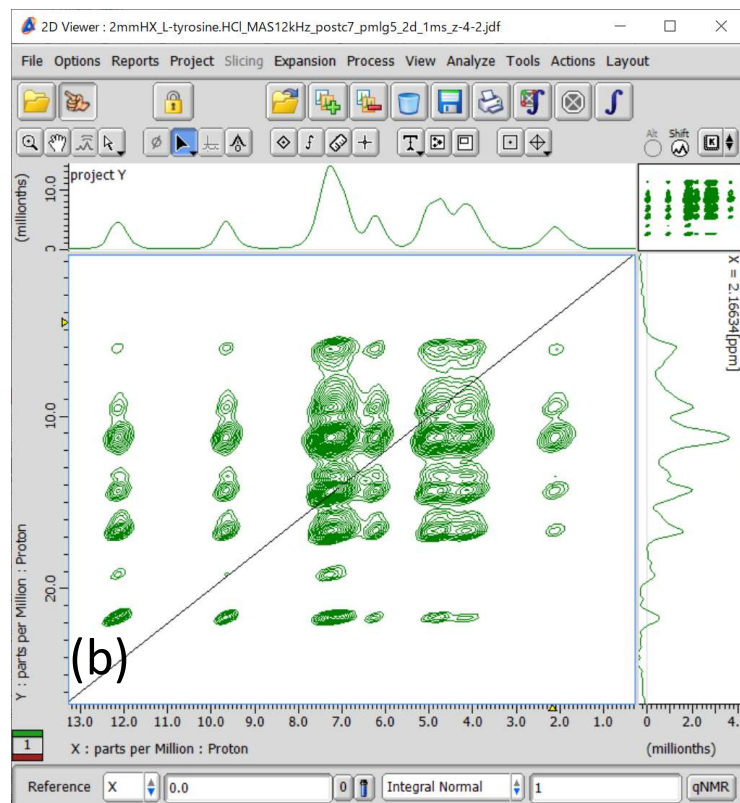
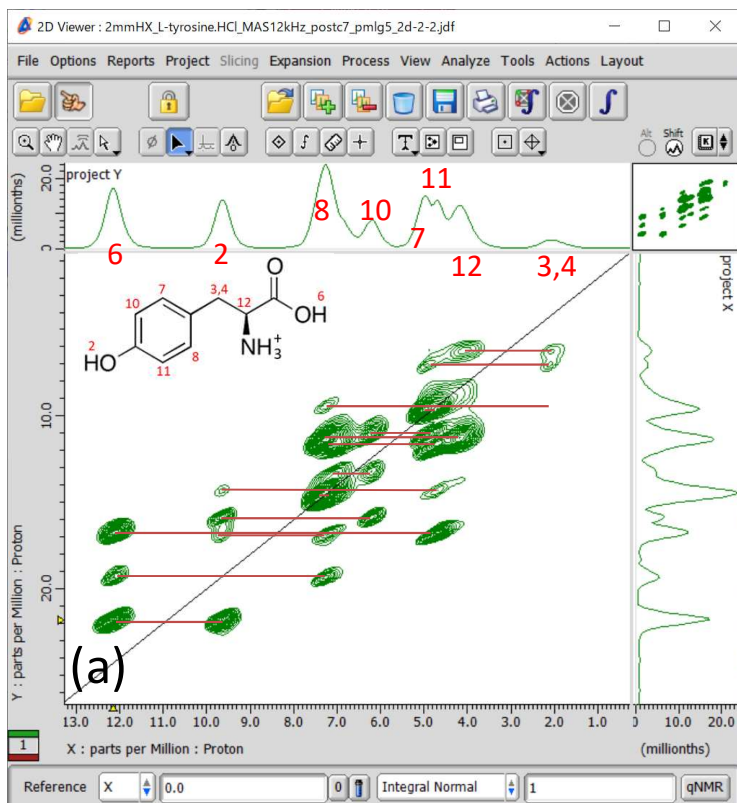


Fig 8. <sup>1</sup>H DQ/<sup>1</sup>H SQ correlation spectra of L-tyrosine.HCl at 12 kHz MAS under 14.1 T without (a) and with (b, 1 ms) z-filtering. Internuclear connectivities are shown with red line in (a). Note that the <sup>1</sup>H assignments are tentative.



**<sup>1</sup>H DQ/ <sup>1</sup>H SQ correlations: data processing (Fig 9)**

The direct dimension is the same as 1D wPMLG. Linear\_Ref and Reference should be applied to correct chemical shift scalings. In the indirect dimension, first peak position has to be shifted with a MAS rate as the peaks appear at +1 SSB (not at the center). This can be done by Reference function. Next Linier\_Ref is applied to re-scale the chemical shift. Note that the spectral center is no longer at 50[%] since we applied reference at the first step. To correct this factor, Center should be set to  $x\_offset * 2$ , which is automatically converted into numeric value depending on the experimental condition used. As the peak position is doubled in the DQ dimension, the parameter used in the subsequent Reference has to be doubled compared to the SQ dimension. Finally, diagonal line is drawn with a slope of 2.

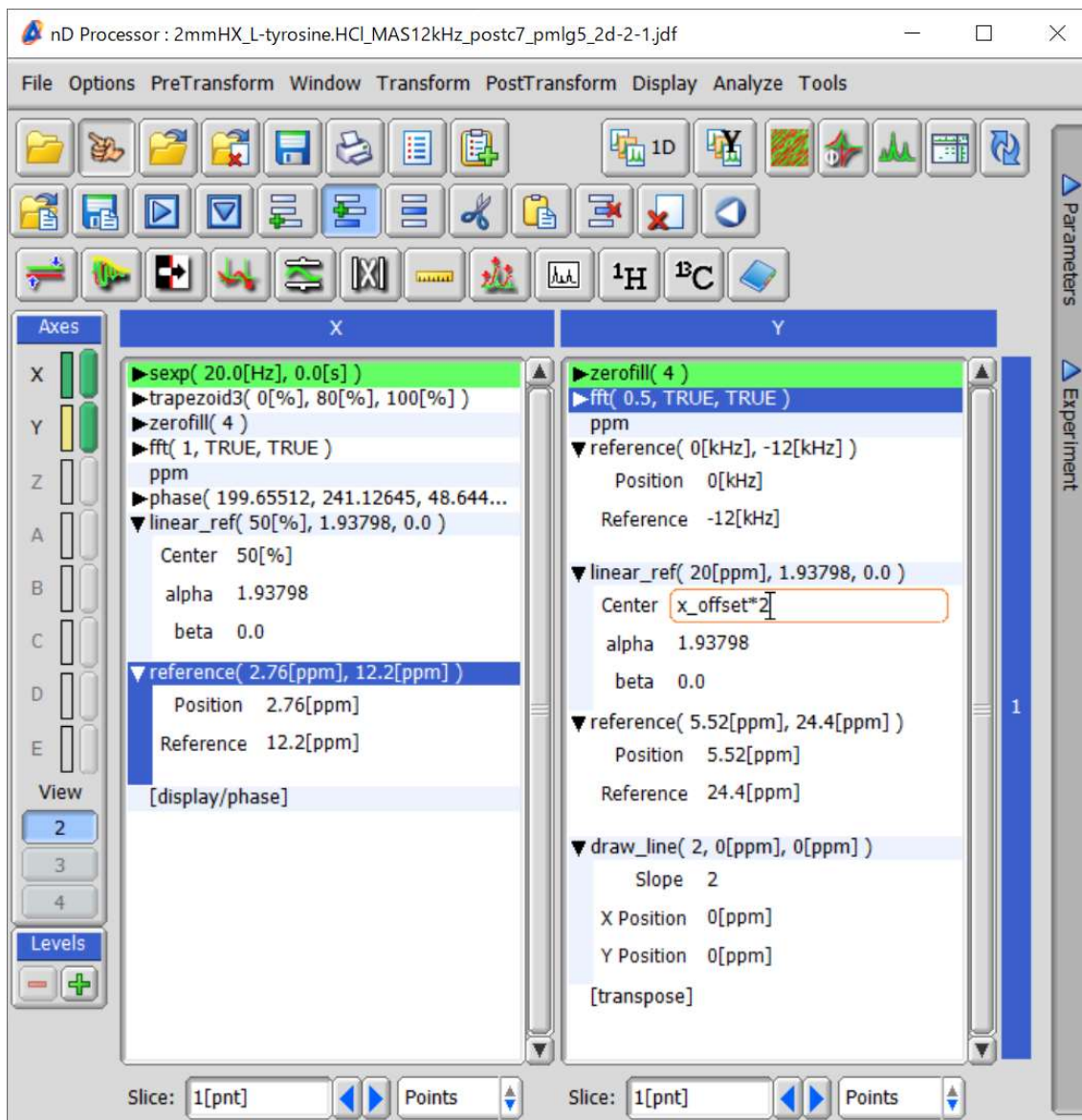


Fig9. Process list used in processing of <sup>1</sup>H DQ/<sup>1</sup>H SQ correlation spectra of L-tyrosine.HCl at 12 kHz MAS under 14.1 T.

The 2D  $^1\text{H}$  DQ/SQ spectrum thus obtained is shown in Fig 8(a). The close look at the spectrum (Fig 10) gives detailed inter nuclear connectivity. H7 and H11, which are overlapped in the 1D dimension are separately observed. The same resolution improvement can be found in H8 and 13 as well. As shown here, DQ/SQ correlation spectra sometimes improve the resolution by adding the DQ dimension.

## Pulse program: postc7\_wpmlg5\_2d.jxp

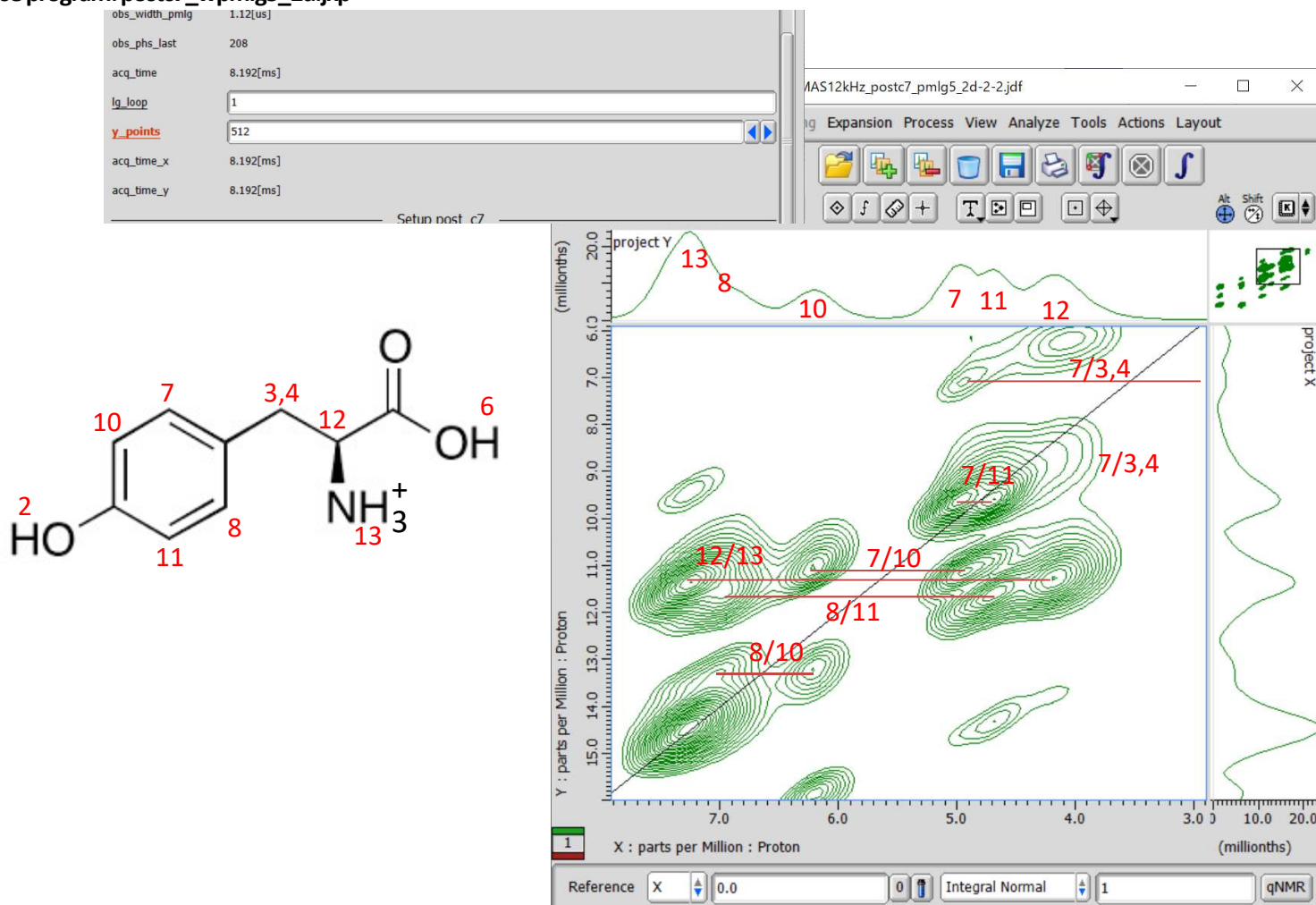


Fig 10. Expansion of  $^1\text{H}$  DQ/ $^1\text{H}$  SQ correlation spectra of L-tyrosine.HCl at 12 kHz MAS under 14.1 T. Whole spectrum is shown in Fig 8(a). Note that the  $^1\text{H}$  assignments are tentative. The increment of the indirect dimension is set to the wPMLG cycle time by putting `Lg_loop` = 1. 512  $t_1$  points were collected with 12 cans for each. The total measurement time was  $512 \times 12 \times 2 \times 1.5$  s (repetition delay) = 5.2 hours.

## References

- [1] S.P. Brown, Prog. Nucl. Magn. Reson. Spectrosc. 50 (2007) 199-251.
- [2] E. Salager, R.S. Stein, C.J. Pickard, B. Elena, L. Emsley, Phys. Chem. Chem. Phys. 11 (2009) 2610-2621.
- [3] J.-N. Dumez, M.C. Butler, E. Salager, B. Elena-Herrmann, L. Emsley, Phys. Chem. Chem. Phys. 12 (2010) 9172-9175.
- [4] N.T. Duong, S. Raran-Kurussi, Y. Nishiyama, V. Agarwal, J. Magn. Reson. 317 (2020) 106777.
- [5] H. Hohwy, H.J. Jakobsen, M. Eden, M.H. Levitt, N.C. Nielsen, J. Chem. Phys. 108 (1998) 2686-2694.
- [6] S.P. Brown, A. Lesage, B. Elena, L. Emsley, J. Am. Chem. Soc. 126 (2004) 13230-13231.
- [7] H. Geen, J.J. Titman, J. Gottwald, H.W. Spiess, J. Magn. Reson. A 114 (1995) 264-267.

Copyright © 2019 JEOL Ltd.

Certain products in this brochure are controlled under the "Foreign Exchange and Foreign Trade Law" of Japan in compliance with international security export control. JEOL Ltd. must provide the Japanese Government with "End-user's Statement of Assurance" and "End-use Certificate" in order to obtain the export license needed for export from Japan. If the product to be exported is in this category, the end user will be asked to fill in these certificate forms.

